JOURNAL OF CATALYSIS 128, 487–498 (1991)

The Effect of Pillaring Montmorillonite and Beidellite on the Conversion of Trimethylbenzenes

M. KOJIMA, R. HARTFORD, AND C. T. O'CONNOR

Department of Chemical Engineering, University of Cape Town, Rondebosch 7700, South Africa

Received February 28, 1990; revised October 11, 1990

Natural montmorillonite, synthetic beidellite, synthetic mica–montmorillonite (SMM), and Ni-substituted SMM were treated with hydroxy–Al solutions and the activities of the respective unpillared and pillared clays were tested using 1,2,4-trimethylbenzene as a reactant. Pillaring montmorillonite and, to a lesser extent, synthetic beidellite gave the largest % increase in the conversion level. The selectivity to 1,2,4,5-tetramethylbenzene, the smallest of the tetramethylbenzene isomers, was found to be a function not of the extent of pillaring, but rather of the extent of isomerization of the alkylbenzenes.

INTRODUCTION

In spite of their relative hydrothermal instability, pillared clays as a class of microporous catalysts continue to attract interest because their effective pore dimensions are larger than those of large pore zeolites. Recently Kikuchi *et al.* (*1, 2*) reported evidence for restricted transition state selectivity in pillared clays for the disproportionation of 1,2,4-trimethylbenzene (124-TrMB). The present study was undertaken to explore further the effect of pillaring a variety of clays on the product distribution for the above reaction. Two classes of clays, one with octahedral and the other with tetrahedral substitutions, viz., montmorillonite and beidellite, were chosen. Pillaring of montmorillonite is well established in the literature, and a comparison of pillared montmorillonite and pillared beidellite has been reported (*3, 4*). In addition, a type of synthetic beidellite which has been demonstrated to be very active even in the unpillared form, viz., synthetic mica–montmorillonite (SMM) and Ni-substituted SMM, were also examined. Unpillared SMM has been shown to be a good acid catalyst for high-pressure propene oligomerization (*5, 6*), but the activity of pillared SMM has not been reported to date. Ni–SMM has been pillared (*7*) with resulting increased catalytic activity.

The above clays were contacted with pillaring solutions to investigate the extent of pillaring on the surface area and the amount of acidity and the catalytic activity of the final clay product. In the case of montmorillonite, attempts were also made to vary the total acidity and pillar density by including Si and Ni, respectively, in the pillaring solution.

EXPERIMENTAL METHODS

Materials

Natural montmorillonite was supplied by Boland Base Minerals Ltd. Its wt% chemical composition as provided by the supplier was 65.1% SiO_2, 20.4% Al_2O_3, 4.8% Fe_2O_3, 2.1% CaO, 4.4% MgO, 0.3% K_2O, and 2.8% Na_2O, and its cation exchange capacity (CEC) was 96 meq/100g. Only particles <2 μm were used for pillaring. Synthetic mica–montmorillonite (SMM) and Ni-substituted synthetic mica–montmorillonite (Ni–SMM) containing 7 wt% Ni were supplied by Harshaw/Filtrol. The latter clay will be designated as Ni(7)-SMM hereafter.

Beidellite was synthesized by using a starting gel obtained by a drop-wise addition

0021-9517/91 $3.00

of a colloidal silica solution to a solution of NaOH and $Al(NO_3)_3 \cdot H_2O$ at 80°C. After the dried gel was calcined at 700°C and ground to a fine powder, the material was redispersed in water and heated at 300°C under autogeneous pressure for 5 days. Ni–SMM containing 21 wt% Ni, designated as Ni(21)–SMM, was synthesized following the procedure described by Gaaf and van Santen (*7*). The nickel content was determined by X-ray fluorescence (XRF). Beidellite, SMM and Ni-SMM in the size range -75 μm were used for the purpose of pillaring.

Pillaring

A hydroxy–Al solution with an OH/Al molar ratio of 1.85 was prepared according to the procedure described by Lahav *et al.* (*8*). Using this hydroxy–Al solution, two solutions of hydroxy–Si/Al with Si/Al mass ratios of 1.0 and 2.0, respectively, were prepared following method B of Sterte and Shabtai (*9*), and a solution of hydroxy–Ni/Al was prepared as described in Shabtai and Fijal (*10*). The latter had a final OH/Al ratio of 2.33 and Al/Ni ratio of 3.55. Prior to pillaring, the clay was dispersed in water (5 g/liter) and stirred overnight. The pillaring solution was added rapidly to the clay suspension which was then stirred for 4 h before being allowed to stand for 20 h. Each gram of clay was contacted with a solution containing 2 mmol Al except in the case of hydroxy Ni/Al solution where 1.7 mmol Al/g clay was used.

Montmorillonite was treated with all the four pillaring solutions. A clay treated with a pillaring solution, whether or not it was successfully pillared, will be designated by first listing the pillaring solution followed by PIL and the clay name. Si/Al(I) PILMont and Si/Al(2) PILMont refer to montmorillonite pillared with hydroxy–Si/Al solutions with Si/Al ratios of 1 and 2, respectively. XRF indicated that Ni/Al PILMont contained 1.7 wt% Ni. If full ion-exchange with the pillaring species is assumed, a nickel content of 1.7% corresponds to a molecular formula of

$$[Al^{IV}(Al_{10.2}Ni_{1.8})^{VI}O_4(OH)_{24}]^{5.2+}$$

for the pillaring species. The addition of Ni to the pillaring solution was investigated to explore the possibility of increasing the pillar density. The amount of Ni initially present in the pillaring solution was twice that measured by XRF in the pillared sample.

All other clays were treated only with the hydroxy–Al solution. To test the reproducibility of the preparation of the hydroxy–Al solution, when SMM, Ni(7)–SMM, and Ni(21)–SMM were pillared, montmorillonite was also treated with the same hydroxy–Al solution under identical conditions in a parallel experiment as a check.

Characterization

For most techniques only particles in the -75 μm size fraction were used, unless otherwise indicated. X-ray diffraction (XRD) patterns were recorded on a Philips diffractometer using Cu$K\alpha$ radiation. Particles were packed into a perspex holder 1 mm deep and the sample surface was oriented by applying pressure with a glass slide. The frontal loading technique (drying a small amount of an aqueous solution of -2 μm particles on a glass slide to ensure a well ordered orientation of particles on the surface of the sample) was carried out as a check on montmorillonite and Al PILNi(7)–SMM. Thermogravimetric analysis (TGA) was performed on 12 to 15 mg of sample using a Stanton–Redcroft STA 780 thermal analyzer. Pillared and unpillared clay samples were heated from room temperature to 750°C in flowing nitrogen at 3°C/min. The propane adsorption capacity of each sample was measured by first heating the sample at 500°C in flowing nitrogen for 4 h and then passing a propane–nitrogen stream (10 ml/min propane and 20 ml/min N_2) dried over 3A molecular sieves over the

sample at 30°C for 6 h. The surface areas of the clay samples were estimated from the results of nitrogen adsorption experiments performed using a Carlo–Erba Sorptometer. Prior to adsorption, samples were outgassed at 110°C for 1 h. The volume of nitrogen adsorbed was measured at between seven and nine different relative pressures in the range 0.01–0.35, and the Langmuir and BET equations were curve fitted to the adsorption isotherms for all samples. Most of the samples were calcined at 500°C for 4 h prior to adsorption.

Ammonia temperature programmed desorption (TPD) was carried out by calcining the sample (size range: 180–250 μm) at 500°C in flowing air for 4 h, passing 4% ammonia/He over the sample at 100°C for 40 min, passing pure He for a further 40 min, and then ramping the temperature at 10°C/min up to 500°C. A TCD was used to detect the amount of ammonia desorbing as a function of temperature, and the desorbing ammonia was also titrated using a H_2SO_4 solution to confirm the total amount of ammonia desorbed. The sample was held at 500°C in flowing He until the TCD signal returned to the baseline. There was excellent agreement between the amount of ammonia desorbed as measured by titration and by TCD.

A ^{27}Al MASNMR spectrum of beidellite was taken on a Brucker AM 300 spectrometer at a spinning speed of 5 kHz.

Reaction

123- and 124-TrMBs were obtained from Aldrich. 135-TrMB was obtained from Merck. Silica–alumina (PK 200) was supplied by Kali-Chemie. The liquid feed was supplied using a syringe pump to a mixing chamber packed with glass beads, where the trimethylbenzene was mixed with a nitrogen stream in a 1 : 1 molar ratio. The tubing and mixing chamber were heated to 220°C. The feed then flowed through the reactor in which 1 g of 106–212 μm catalyst particles was packed, and into a double stage condenser surrounded by a cooling jacket through which cold water was circulated. Clay samples were calcined at 500°C in air for 10 h. The reactor temperature was then allowed to cool to 300°C and the feed was passed at a WHSV of 2.4 h^{-1} unless otherwise indicated. Liquid product was collected at 15 min intervals and analyzed immediately using an HP 5890 A gas chromatograph fitted with a Supelcowax 10 fused silica 0.2 mm × 30 m capillary column. The response factors for all the aromatic compounds were set equal to unity. Mass % isomerization was based on the amount of the two other isomers of TrMB present in the product relative to the amount of the reacted feed.

124-TrMB was reacted over all the clay samples. In addition, 123- and 135-TrMBs were reacted over SMM and Si/Al(1) PILMont.

RESULTS

Clay Synthesis and Pillaring

Figure 1 shows XRD spectra of Ni(21)–SMM and Ni(7)–SMM. The peaks at 7.2 and 3.53 Å observed only in Ni(21)–SMM may indicate the presence of impurity, possibly Ni–serpentine (*11*). Beidellite and SMM are structurally identical, and hence their XRD spectra should be similar. Indeed, as shown in Fig. 2, this was found to be the case. Differences in the positions of the basal peaks are attributed to different amounts of tetrahedrally coordinated Al in the two clays. This affects the charge deficit on the clay lattice which in turn governs the extent of swellability of the layers and the interlayer spacings. ^{27}Al MASNMR gave three peaks near 0, 50, and 70 p.p.m. The height of the peak at 70 p.p.m. was large, indicating a fair degree of tetrahedral substitution. The peak at 50 p.p.m. suggests the presence of nonoctahedral extraframework Al.

Table 1 shows the positions of the 001 peaks of the pillared and unpillared clays. The 001 peak of montmorillonite was well defined and represented a basal spacing of

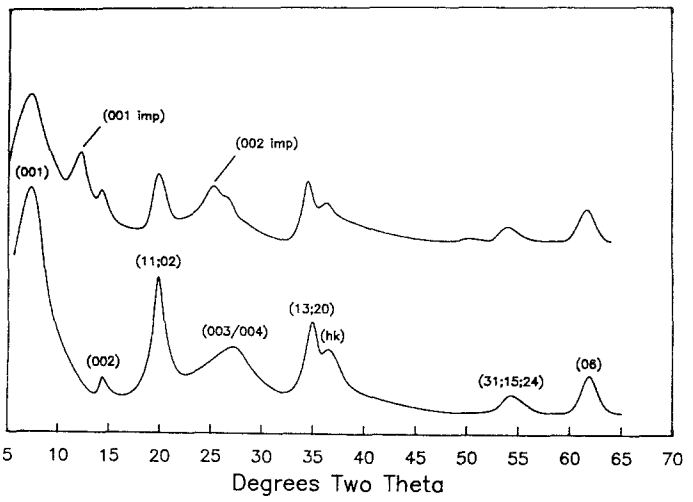

FIG. 1. XRD patterns of Ni(21)–SMM (top) and Ni(7)–SMM (bottom); "imp" denotes possible presence of clay impurity.

13.3 Å. Treating montmorillonite with various pillaring solutions all resulted in a decrease in the 2θ value, indicating an expanded basal spacing of greater than 19 Å. The basal spacing of 17.5 Å observed after calcination at 500°C corresponds to an interlayer spacing of 7.9 Å. The XRD spectra of montmorillonite pillared here and in the control experiments (carried out during pillaring of SMM and Ni–SMM as described in the experimental section) were all identical and indicated that the pillaring procedure was reproducible.

The 001 peak of beidellite was also well defined. Upon pillaring, the original 001 basal peak shifted to give an interlayer spacing of 9.9 Å before calcination.

When the additivity relationship sug-

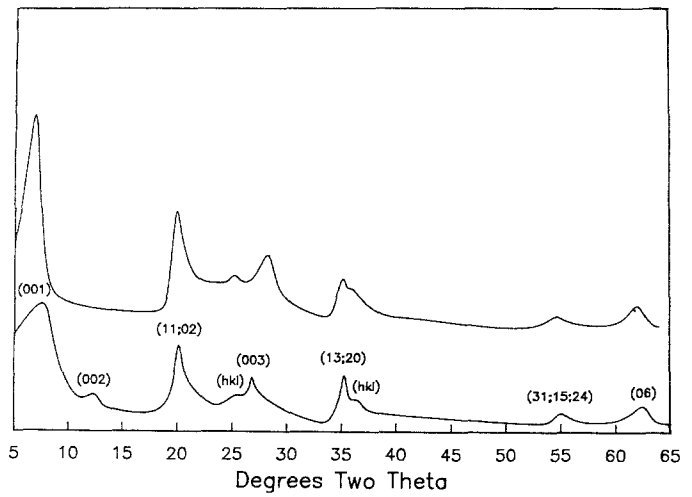

FIG. 2. XRD patterns of beidellite (top) and SMM (bottom).

TABLE 1

XRD 001 Basal Peak Positions of Pillared and Unpillared Clays before and after Calcination at 500°C

Clay	Uncalcined (Å)	Calcined (Å)
Montmorillonite	13.3	n.a.
Al PILMont	19.5	17.5
Si/Al PILMont	19.3	17.6
NI/Al PILMont	19.2	17.6
Beidellite	12.8	n.a.
Al PILBeid	19.4	18.1
SMM	11.4	9.8
Al PILSMM	10.4; 20.5	9.8; 19
Ni(7)–SMM	12.1	9.8
Al PILNi(7)–SMM	—	—
Ni(21)–SMM	12.1; 7.2	7–10
Al PILNi(21)–SMM	7.2	7.2

Note. n.a. = not available.

gested by Granquist (*12*) was applied to the 001 peak position of 11.4 Å observed in unpillared SMM, SMM was found to contain 59% mica-like material in the present work. Hence this clay should be regarded as being approximately 40% swellable. Pillaring gave rise to two peaks, the one at 10.4 Å corresponding to the basal spacing in the mica-like material and the other at 20.5 Å corresponding to that in the pillared portion. In contrast, pillaring Ni(7)–SMM resulted in the generation of a very diffuse spectrum in the region where the basal peaks appear. The original peak at 12.1 Å disappeared completely, and no peak was detected at a lower value of 2θ to indicate the presence of an expanded-layer structure, nor was there a peak near 10 Å corresponding to the non-swellable portion of the clay. Calcination of Ni(21)–SMM resulted in the disapperance of the peak at 12.1 Å and the appearance of a broad band in the region of 7–10 Å. As in the case of Ni(7)–SMM, treating Ni(21)–SMM with a pillaring solution yielded a very diffuse spectrum in the region where the first order basal peaks appear. The only clearly discernible 001 peak was at 7.2 Å. This was assigned to the Ni–serpentine which was postulated to be present in this clay.

TGA showed that during calcination pillared clay samples lost more weight than their unpillared counterparts. More specifically, Na montmorillonite lost little weight between 150 and 500°C, while PILMont showed a steady weight loss between 150 and 700°C. The increase in weight loss upon treatment with pillaring solutions was the smallest in the case of Ni(21)–SMM.

The results of surface area measurements by means of nitrogen adsorption are shown in Table 2. In the case of montmorillonite, beidellite, and SMM, the BET equation gave a linear plot prior to pillaring, while subsequent to pillaring the Langmuir equation gave a far more linear plot than the BET equation. The surface area of montmorillonite increased markedly upon pillaring whereas the increase in the surface area of beidellite was not nearly as large. In the case of Ni–SMM, it was not clear that there was any increase in the surface area upon pillaring. Moreover, particularly in the case of Ni(21)–SMM, the BET equation gave a more linear plot even after pillaring.

Table 3 gives % weight gain expressed as a percentage of the calcined mass of catalyst after passing propane at 30°C for 6 h. The weight increase was extremely rapid during the first hour, and leveled off subsequently. The equilibrium was not reached within 6 h, and hence the figures given indicate the amount of uptake achieved after 6 h. Pillared montmorillonite samples had much greater propane adsorption capacities than the parent clay. The weight increase was less for Ni/Al PILMont than the other two pillared montmorillonite samples.

The amount of ammonia desorbing between 100 and 500°C during TPD obtained by integrating the area under the desorption spectrum and the amount of ammonia thus obtained normalized with respect to surface area in m^2 are shown in Table 4. For all the samples the desorption maximum was near 200°C. Pillaring increased substantially the amount of ammonia desorbing near 200°C in the case of beidellite, and to a lesser extent SMM and montmorillonite. TPD was also carried out on Si/Al(2) PILMont calcined at

TABLE 2

Surface areas (m^2/g) and BET and Langmuir Isotherm Equation Correlation Coefficients of Clays Calcined at 500°C

Catalyst	BET		Langmuir	
	r^2	Surface area	r^2	Surface area
NH_4 Mont	0.9957	23	0.9746	(31)
Al PILMont[a]	0.9979	(250)	0.9997	343
Al PILMont	0.9982	(189)	1.0000	237
Si/Al(2) PILMont	0.9985	(173)	0.9999	227
Ni/Al PILMont	0.9955	(177)	0.9994	253
NH_4 Beid	0.9998	117	0.9992	(143)
Al PILBeid[a]	0.9985	(156)	0.9997	198
Al PILBeid	0.9959	(132)	0.9987	163
SMM[a]	0.9999	120	0.9930	(166)
SMM	0.9994	101	0.9982	(135)
Al PILSMM	0.9983	163	0.9999	215
Ni(7)–SMM[a]	0.9996	222	0.9947	(295)
Ni(7)–SMM	1.0000	185	0.9977	(245)
Al PILNi(7)–SMM	0.9989	190	0.9988	168
Ni(21)–SMM[a]	1.0000	163	0.9957	(220)
Ni(21)–SMM	0.9998	151	0.9940	(211)
Al PILNi(21)–SMM	0.9995	150	0.9950	(201)

[a] Uncalcined

300, 400 and 500°C. The differences in the TPD spectra were within experimental error. Although beidellite and SMM had comparable BET surface areas and propane adsorption capacities, the amounts of acidity differed substantially between the two clays.

TABLE 3

Propane Adsorption at 30°C, 6 h

Sample	Wt% gain
Na montmorillonite	0.4
Al PILMont	3.2
Si/Al(2) PILMont	2.9
Ni/Al PILMont	2.0
Na beidellite	0.6
Al PILBeid	1.8
SMM	0.5
Al PILSMM	2.2
Ni(7)–SMM	1.1
Al PILNi(7)–SMM	3.3
Ni(21)–SMM	0.9
Al PILNi(21)–SMM	1.7

Reaction

The total conversion of 124-TrMB as a function of time on stream before and after pillaring is illustrated in Figs. 3–5. The con-

TABLE 4

Ammonia TPD Results: mmol Ammonia/g Clay Desorbed as Measured by TCD and μmol Ammonia/m^2 Clay Surface

Sample	mmol/g	μmol/m^2
NH_4^+ Mont	0.07	3.04
Al PILMont	0.22	0.93
Si/Al(1) PILMont	0.22	
Si/Al(2) PILMont	0.23	1.01
Ni/Al PILMont	0.22	0.87
NH_4^+ Beid	0.04	0.34
Al PILBeid	0.14	0.86
SMM	0.17	1.68
Al PILSMM	0.25	1.16
Ni(7)–SMM	0.20	1.08
Al PILNi(7)–SMM	0.31	1.63
Ni(21)–SMM	0.24	1.59
Al PILNi(21)–SMM	0.36	2.40

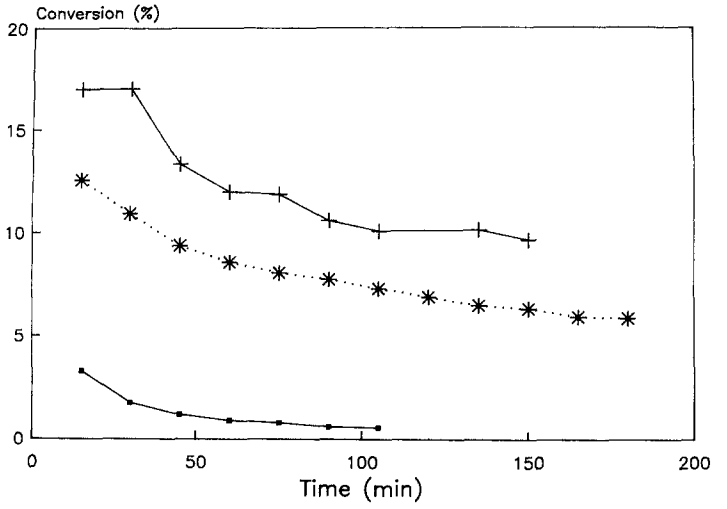

FIG. 3. % conversion of 124-TrMB vs. time on stream; (+) Al PILMont, (*) Ni/Al PILMont, (■) NH_4 Mont.

version versus time plots of Si/Al(1) and Si/Al(2) PILMont were essentially identical to that of Al PILMont shown in Fig. 3. Only Ni/Al PILMont had a lower activity level than the other pillared montmorillonite samples. In terms of total activity, SMM was the most active clay, both in pillared and unpillared forms. The rate of deactivation did not increase markedly upon pillaring except in the case of Al PILNi(21)–SMM. There was little dealkylation in all the cases. The % disproportionation decreased gradually while the % isomerization increased in the case of unpillared SMM, Ni(7,21)–SMM, and silica–alumina, while they were essentially independent of time on stream for pillared clays. Table 5 shows the initial and final % total conversion, aver-

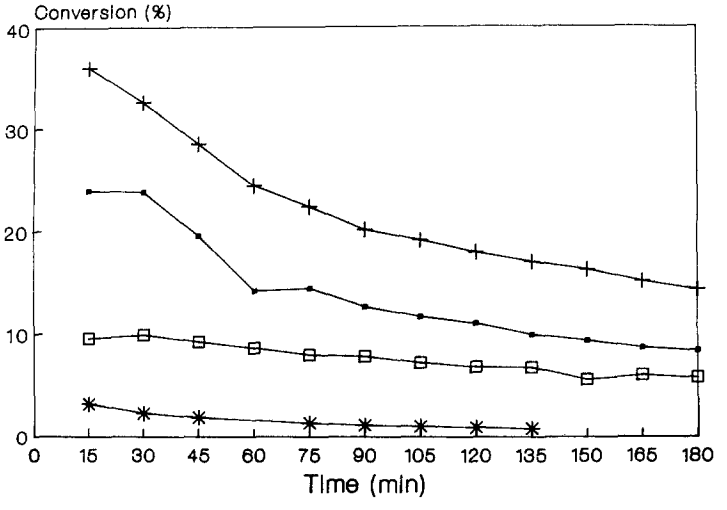

FIG. 4. % conversion of 124-TrMB vs. time on stream; (+) Al PILSMM, (■) NH_4 SMM, (□) Al PILBeid, (*) NH_4 Beid.

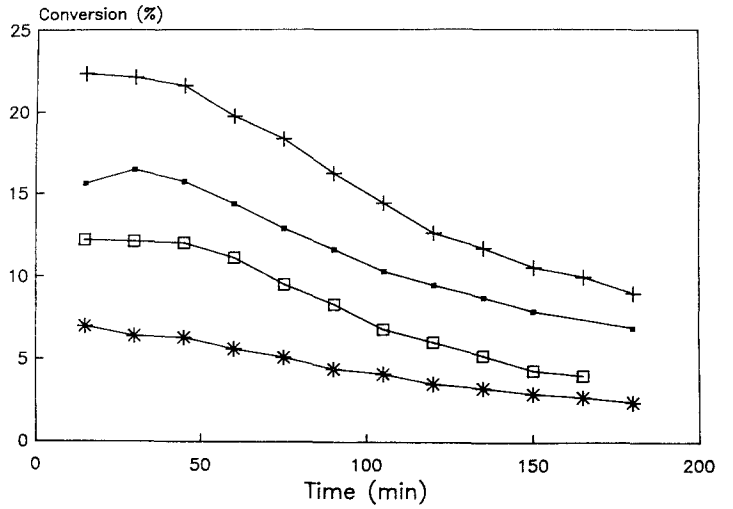

FIG. 5. % conversion of 124-TrMB vs. time on stream; (+) Al PILNi(7)–SMM, (■) NH_4 Ni(7)–SMM, (□) Al PILNi(21)–SMM, (*) NH_4 Ni(21)–SMM.

aged % of the converted 124-TrMB which isomerized, the composition of the TrMB isomers other than 124-TrMB detected in the effluent, and % of tetramethylbenzenes (TeMB) which constituted 1245-TeMB at the beginning and the end of each run. 1245-TeMB selectivities tended to increase, and 1235-TeMB selectivities tended to decrease, with time on stream, while 1234-TeMB selectivities were fairly constant. In all the cases, the average xylene compositions were essentially independent of the clay structure and varied between 43 and 46% for *m*-xylene and 38 and 42% for *o*-xylene. There was a slight decrease in *p*- and *m*-xylene selectivities and a slight increase in *o*-xylene selectivity during the first half hour on stream. It should be noted that in every run both 1245-TeMB and *o*-xylene selectivities were much higher than the thermodynamic equilibrium compositions (53% *m*-xylene, 23% *o*-xylene, and 24% *p*-xylene; 52% 1235-, 35% 1245-, and 13% 1234-TeMB).

To test the effect of conversion on selectivities, 124-TrMB was passed over SMM at a WHSV of 8 h^{-1}. This decreased the initial conversion from 24 to 14%, decreased initial isomerization from 24 to 22%, and increased initial 1245-TeMB from 45 to 48%. In another run the WHSV was increased from 2.4 to 5 h^{-1} over Al PILMont. This decreased the initial conversion from 18 to 11%, initial isomerization from 13 to 10%, and increased 1245-TeMB from 59 to 64%. Thus % isomerization and % 1245-TeMB were a greater function of catalyst formulation than of % conversion.

Since the extent of isomerization was computed from the amount of 123- and 135-TrMB present in the product and this does not take into account the isomers which have subsequently disappeared by disproportionation, 123- and 135-TrMB were also reacted over Al PILMont and SMM to see their reactivities. The results are summarized in Table 6. Predictably, the % isomerization was much greater for 123- and 135-TrMB than for 124-TrMB. The overall reactivities of these isomers were comparable to that of 124-TrMB, and thus % isomerization computed in the present study should reasonably reflect the actual extent of isomerization in that the other two isomers of TrMB were not significantly more active for disproportionation.

DISCUSSION

The results of all the characterization techniques indicated that montmorillonite was pillared successfully. The weight gain

TABLE 5

Conversion of 124 Trimethylbenzene

Catalyst	% conversion	% isom.	% 134-TrMB	% 123-TrMB	% 1245-TeMB
NH_4^+ Mont	3.3–0.6	5.9	59	41	72–74
Al PILMont	17–9.7	12.1	54	46	59–64
Si/Al(1) PILMont	20–8.6	14.3	56	44	57–62
Si/Al(2) PILMont	17.5–9.3	13.9	54	46	57–62
Ni/Al PILMont	12.5–8.3	8.3	53	47	65–71
NH_4^+ Beid	3.2–0.8	9.9	55	44	68
Al PILBeid	9.6–5.8	9.8	53	47	66–68
SMM	24–8.4	30.7	63	37	45–50
Al PILSMM	36–15	21.3	62	39	45–52
Ni(7)–SMM	16.5–6.9	17.3	56	44	57–62
Al PILNi(7)–SMM	22–9	17.7	57	43	55–60
Ni(21)–SMM	7–2.5	8.4	55	45	69–72
Al PILNi(21)–SMM	12–2.4	11.3	55	45	61–67
silica–alumina	27.5–20	35.9	62	38	45–46

subsequent to propane adsorption suggests that the pillar density may be higher in Ni/Al PILMont. TPD gave values of μmol ammonia/m^2 for Al and Si/Al PILMont which were more lower than those given by Sterte and Shabtai (*9*). In contrast to their findings, there was no evidence that the amount of acidity increased upon introduction of Si into the pillaring solution. The surface area of beidellite was similar to 107 m^2/g for the beidellite synthesized by Plee *et al.* (*3*). However, in the latter study the surface area upon pillaring and after degassing at 220°C increased to 319 m^2/g while here the increase was only about 50%. The amount of acidity present on beidellite was much smaller than that of SMM which had a comparable surface area. One possible explanation is a lower charge density on the beidellite.

XRD indicated that the swellable portion of SMM was pillared. In contrast, it is not at all clear from XRD that any pillaring took place on Ni–SMM. The XRD spectrum of

TABLE 6

Comparison of Reactivities of the Three Trimethylbenzene Isomers over SMM and Si/Al(1) PILMont

Reactant	% Conversion		% Isom.	% tetMB			% Xylene	
	initial	90 min		1245	1235	1234	*o*-	*m*-
			Si/Al(1) PIL Mont					
123	15[a]	7[a]	50[a]	19.3	61.1	19.5	60.4	36.9
134	9	2	68	22.7	69.6	7.5	[b]	[b]
124	20	11	14	58.7	33.9	7.4	39.4	46.8
			SMM					
123	35[a]	18[a]	68[a]	32.7	54.1	13.2	53.3	40.5
135	22	7	75	34.5	56.7	8.9	[b]	[b]
124	24	13	28	47.2	43.6	9.2	37.1	48.1

[a] 124-TrMB present as feed impurity (2.3 mass%).
[b] *o*-xylene present as feed impurity (4.4 mass%).

Ni(21)–SMM indicated the presence of Ni–serpentine. This two-layer structure has no swellable property. The diffuse nature of the XRD spectra may suggest extensive delamination rather than pillaring. This postulate is supported by a comparison of the relative linearities of the BET and Langmuir isotherm equations. The BET equation gave a far more linear relationship in the case of Al PILNi(21)–SMM, and the same degree of linearity as the Langmuir equation in the case of Al PILNi(7)–SMM. Further delamination should result in increased acidity as detected by ammonia TPD and increased propane adsorption capacities. However, it is difficult to explain why the surface area hardly changed if further delamination occurred.

Contacting clay samples with pillaring solutions increased the TrMB conversion level in all cases. The increase in activity of Ni/Al PILMont was the smallest of all the pillared montmorillonite samples. This provides further evidence that the pillar density in Ni/Al PILMont may be greater. There was no direct relationship between the amount of acidity measured during TPD and the overall catalyst activity. In particular, Ni(21)–SMM which had as much acidity according to ammonia TPD as Al PILSMM yielded only 20% of the activity of the latter catalyst. Even taking into account the difference in the surface area or the propane adsorption capacity, the activity level of Ni(21)–SMM was low.

Little dealkylation was observed to be taking place, and hence it follows that a reaction mechanism involving a bimolecular transition state is probably operative. Kikuchi *et al.* (*1*) attributed high 1245-TeMB and *o*-xylene selectivities over pillared clays to restricted transition state selectivity introduced by pillars. This hypothesis however cannot explain the data in the present study. If transition state selectivity governs the product distribution, PILMont should show the highest 1245-TeMB selectivity. Instead, two unpillared clays, montmorillonite and Ni(21)–SMM, gave the highest 1245-TeMB selectivities. An examination of Table 5 readily suggests that the selectivity towards the formation of 1245-TeMB was correlated not with the extent of pillaring but with the extent of isomerization. Indeed, a comparison of the results of reaction over HY and over pillared clays in Kikuchi *et al.* (*2*) demonstrates that as the extent of reactant isomerization increased, the selectivity towards 1245-TeMB decreased. More specifically, HY, which had the highest % isomerization, gave the lowest 1245-TeMB selectivity. If transition state selectivity is responsible for high conversion to 1245-TeMB, HY should show one of the highest 1245-TeMB compositions.

There are three factors which should be considered in explaining the results of this reaction. They are:

(i) the stability of the reaction intermediate;
(ii) the steric hindrance introduced by the presence of methyl groups;
(iii) the size of the reaction intermediate.

Specifically factor (ii) considers the number of methyl groups in positions marked by *:

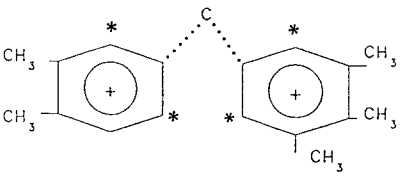

If a large fraction of the four positions are occupied by methyl groups, there will be a large degree of steric hindrance and such an intermediate will not be easily formed. This will indeed be the case provided that the aromatic ring orients itself parallel to the catalyst surface so that rotation around the C-phenyl bond is unlikely to occur. The assumption of parallel orientation is reasonable given the strong interaction which will exist between the conjugated double bonds of the aromatic ring and the surface acid sites. Indeed, the intermediate identified by Kikuchi *et al.* (*1*) as most abundant had only one of the four positions occupied by a methyl group.

Kikuchi *et al.* (*1*) considered factors (i) and (iii) for disproportionation between two 124-TrMB molecules and came to the conclusion that (iii) was the determining factor. However, it is clear that the results of this study cannot be explained by their reasoning.

A more satisfactory reasoning should be able to explain the constant *o*-xylene selectivity irrespective of catalyst formulation, and the close correlation between isomerization and 1245-TeMB selectivities. The observation that the higher the extent of reactant isomerization the lower the selectivity towards 1245-TeMB formation may be explained in part by postulating that the extent of isomerization of the product TeMB is also high on those catalysts which are active for reactant isomerization. Hence the product composition will shift more towards the thermodynamic equilibrium. However, for the hypothesis of restricted transition state selectivity to hold, an additional assumption must be made that over pillared clays a greater quantity of 1245-TeMB is formed initially which is subsequently isomerized. Moreover, this explanation cannot explain the constant *o*-xylene selectivity.

Aside from disproportionation between two 124-TrMB molecules, another reaction which should be considered is "cross-disproportionation," viz., the disproportionation between 124-TrMB and another TrMB isomer formed by reactant isomerization. By considering the case in which 124-TrMB is protonated and donates a methyl group to 135- or 123-TrMB, it is clear that 1245-TeMB cannot be formed. If 135- and 123-TrMB is protonated and donates a methyl group to 124-TrMB, then all three isomers of TeMB can be formed. None of the intermediates arising from these combinations have dimensions as small as the one identified by Kikuchi *et al.* (*1*) to be the most abundant intermediate which could take advantage of shape selectivity. Hence if shape selectivity was a determining factor, then "cross-disproportionation" should not occur to any appreciable extent. Yet as noted previously, isomerization had a marked effect on 1245-TeMB selectivities. This suggests that factors (i) and (ii) are more important than factor (iii).

An examination of the resonance structures of all the intermediates formed during "cross-disproportionation" shows that the most stable is

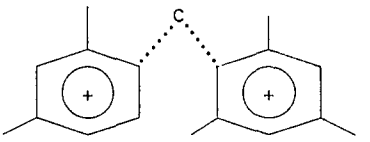

which gives rise to *m*-xylene and 1235-TeMB. However, from the viewpoint of (ii), the most favourable is

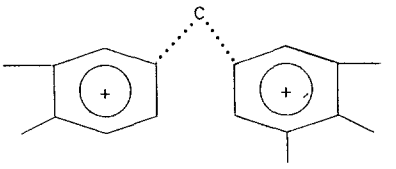

which leads to the formation of *o*-xylene and 1235-TeMB. While in terms of resonance structures this intermediate is one of the least stable, this can explain the decrease in 1245-TeMB selectivity as a result of isomerization as well as the constant *o*-xylene selectivity.

There are five intermediates which have only one methyl group occupying the four starred positions indicated in the figure above. The two most stable carbonium ion intermediates of the five are

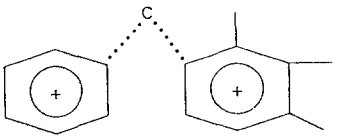

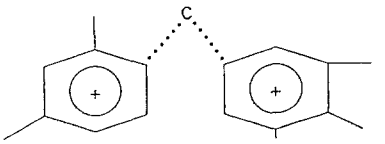

which lead to the formation of *o*-xylene and 1234-TeMB, and *m*-xylene and 1235-TeMB,

respectively. Either reaction pathway will decrease the selectivity towards 1245-TeMB, while the former will contribute to the excess of *o*-xylene.

From the foregoing discussion, it is suggested that one explanation which is consistent with the data obtained in this study as well as those of Kikuchi *et al.* (*1*, *2*) is that which gives abundant intermediates as those with little crowding of methyl groups. Kikuchi *et al.* (*2*) pointed to the order of reactivity of TrMB as further evidence of restricted transition state selectivity, that is, 123-TrMB which is the least stable should be most reactive over unpillared clays, while 124-TrMB which is the smallest should be most reactive over pillared clays. While a similar reactivity order was observed in the present study, it is difficult to attribute this trend to shape selectivity. The dimensions available even inside pillared clays are much larger than those of TrMB, and particularly for monomolecular reactions (isomerization possibly being such a reaction), it is difficult to visualize transition state shape selectivity as a governing factor. Indeed, Occelli *et al.* (*13*) have reported that the transport of 135-TrMB occurs with ease in pillared bentonite.

CONCLUSIONS

Treating Ni–SMM with a hydroxy–Al solution appeared to result in further delamination rather than pillaring. The highest conversion of 124-TrMB was obtained over SMM. The disproportionation product distribution appeared to be governed not by shape selectivity introduced by pillars, but by steric hindrance owing to the presence of methyl groups near the penta-coordinated carbon atom in the intermediate species.

ACKNOWLEDGMENTS

The authors wish to thank the University of Cape Town, Sasol and the Foundation for Research Development for financial assistance, AECI for carrying out nitrogen adsorption measurements, Harshaw/Filtrol Corporation in the USA for the supply of SMM and Ni–SMM, and Kali-Chemie AG in the FRG for the supply of silica–alumina.

REFERENCES

1. Kikuchi, E., Matsuda, T., Fujiki, H., and Morita, Y., *Appl. Catal.* **11,** 331 (1984).
2. Kikuchi, E., Matsuda, T., Ueda, J., and Morita, Y., *Appl. Catal.* **16,** 401 (1985).
3. Plee, D., Gatinequ, L., and Fripiat, J. J., *Clays Clay Miner.* **35,** 81 (1987).
4. Diddams, P. A., Thomas, J. M., Jones, W., Ballantine, J. A., and Purnell, J. H., *J. Chem. Soc. Chem. Commun.* 1340 (1984).
5. Fletcher, J. C. Q., Kojima, M., and O'Connor, C. T., *Appl. Catal.* **28,** 181 (1986).
6. O'Connor, C. T., Jacobs, L. L., and Kojima, M., *Appl. Catal.* **40,** 277 (1988).
7. Gaaf, J., and van Santen, R., European Patent No. 0 090 442 (1983).
8. Lahav, N., Shani, U., and Shabtai, J., *Clays Clay Miner.* **26,** 107 (1978).
9. Sterte, J., and Shabtai, J., *Clays Clay Miner.* **35,** 429 (1987).
10. Shabtai, J., and Fijal, J., US Patent 4 579 832 (1986).
11. Feitknecht, W., and Berger, A., *Helv. Chim. Acta* **25,** 1543 (1942).
12. Granquist, W., US Patent 3 252 757 (1966).
13. Occelli, M. L., Innes, R. A., Hwu, F. S. S., and Hightower, J. W., *Appl. Catal.* **14,** 69 (1985).